Dual Function Trade-off in Joint Communications and Radar: An Electromagnetic Field Analysis

Husheng Li

***Abstract*— Joint communications ad radar (JCR) is a technology to leverage the same waveform for simultaneous data transmission and radar sensing, which is expected to be efficient in bandwidth and power. A theoretical framework is proposed to study JCR, based on the electromagnetic field analysis. Given a simple model of communications and radar sensing, the electromagnetic field is described in terms of forward and scattering Green functions. For radar sensing, the imaging error is derived based on the Fisher operator and the eigen-decomposition of the integral transformations with Green function kernels. For data transmission, the channel capacity is analyzed based on a similar eigen-decomposition. The trade-off between the imaging error of radar and the channel capacity of data transmission is obtained based on the theoretical analysis and numerical computations.**

I. Introduction

Communications and radar are both important applications of electromagnetic (EM) field. Due to the different historic origins and hardware constraints, traditional communication and radar systems are developed independently. In typical situations, they use different frequency bands and are operated separately (e.g., the 10.525GHz band is used for police radar, while the 28GHz is used for 5G communications). However, there is a pressing need to integrate both communications and sensing in a single EM platform, sharing the same frequency band and even the same waveform, thus improving the efficiencies of frequency spectrum and power. For example, in vehicular networks, a vehicle may send communication signal to another nearby vehicle for delivering messages; meanwhile, the emitted EM wave is reflected by a target and carries information about the target (e.g., the range and the velocity). Meanwhile, when a vehicle sends out sensing signals to detect nearby vehicles, the waveform can be modulated, such that some system information (e.g., the location and velocity of the vehicle itself) can be broadcasted to other vehicles. A general situation of such a joint communications and radar (JCR) is illustrated in Fig. 1. Note that, the communication receiver and the sensed target could be co-located, while the JCR transceiver could have separated transmitter and receiver (similarly to a bi-static radar).

H. Li is with the Department of Electrical Engineering and Computer Science, the University of Tennessee, Knoxville, TN (email: husheng@eecs.utk.edu

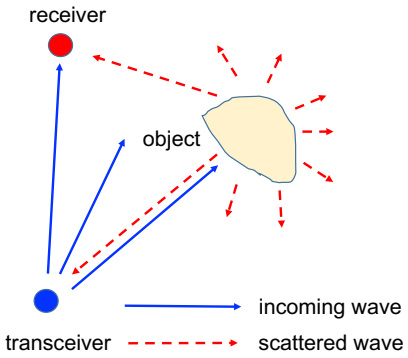

Fig. 1: Illustration of incoming and scattered waves in JCR system.

The integration of communications and radar sensing has been studied for a long time [1]–[4]. In particular, there has been a resurrection on this topic in recent years, due to the pressing need in efficient spectrum access. However, there has not been a systematic study, ranging from theoretical foundations to practical system designs, in this area. In particular, a fundamental challenge on JCR is how to understand the roles of bandwidth and power, which are the two basic resources for both communications and sensing, as well as the trade-off between performances of communications and radar. In particular, one wants to known whether communications and radar have significant conflict with each other (thus better to separate) or not (thus better for joint operation). We have carried out experimental studies on this topic in [5], based on existing frequency modulation continuous waveform (FMCW) millimeter wave radar. In this paper, we analyze the performances of data communications and radar imaging using the EM field framework, and explore the fundamental trade-off between radar and communications. The analysis is based on the eigen-decomposition of integral transformations related to EM waves, which converts the continuous field to discrete numbers and facilitates the analysis. Note that this paper focuses on only the radar imaging, while radar ranging and Doppler estimation are analyzed in our other publications.

For related researches, comprehensive surveys on JCR can be found in [6]–[9]. For the EM field in communication networks, the degrees-of-freedom analysis has been carried

out in [10]–[12], in which the number of ϵ-distinguishable EM fields is calculated as a function of the scatterer dimensions. The approach of EM field cut-set analysis on network capacity has been used in [11], [13], [14] to obtain the scaling law for communication throughput and radar sensing accuracy. Although this paper does not follow the approach of degrees-of-freedom, the basic laws of EM field and the eigen-decomposition of integral transform are the same.

The remainder of this paper is organized as follows. The system model is introduced in Section II. The performances of radar and communications are analyzed in Sections III and IV, respectively. Numerical results are provided in Section V. Finally, conclusions are drawn in Section VI.

II. System Model

In this section, we introduce the system model, particularly the EM field model for the subsequent analysis.

A. Communications and Radar

We consider a communication/radar transmitter, a radar receiver, a communication receiver, and a sensing target. It is possible that the communication receiver is also the radar target (e.g., vehicle A senses vehicle B while transmitting a message to it). The radar receiver could be located at the transmitter (thus forming a JCR transceiver), or at a different location. The regions of the transmitter antenna, communication receiver, radar receiver and target are denoted by Ω_t, Ω_r, Ω_x and Ω_o, respectively.

B. EM Field Modeling

Now we model JCR in terms of EM field, which is fundamental for the analysis of JCR performance.

1) EM Wave: The real-valued radiated wavefield of EM is described by the following inhomogeneous scalar wave equation:

$$\left[\nabla^2 - \frac{1}{c^2}\frac{\partial^2}{\partial t^2}\right] u(\mathbf{r},t) = q(\mathbf{r},t), \tag{1}$$

where ∇^2 is the Laplacian, c is the light speed, u is the scalar potential, $\mathbf{r}$ is the three-dimensional coordinate, and q is the time-varying charge source. Taking the Fourier transform on (1), we obtain the scalar Helmholtz equation:

$$\left[\nabla^2 + k^2\right] U(\mathbf{r},w) = Q(\mathbf{r},w), \tag{2}$$

where U and Q are the Fourier transforms of u and q, respectively, w is the angular frequency (in terms of radians), and k is the wave number.

2) Propagation and Scattering: For notational simplicity, we omit the argument w in U and Q by considering a monochromatic EM field. For free space, the solution to the Helmholtz equation is given by

$$U(\mathbf{r}) = \int_{\Omega_t} G_+(\mathbf{r},\mathbf{r}')Q(\mathbf{r}')d\mathbf{r}' \tag{3}$$

where $G_+(\mathbf{r}',\mathbf{r})$ is the forward Green function, which is essentially the response at position r given an impulse input at position $\mathbf{r}'$. It is well known that the Green function in the free space is given by (page 10, [15])

$$G_+(\mathbf{r},\mathbf{r}') = G_+(\mathbf{r}'-\mathbf{r}) = -\frac{1}{4\pi}\frac{e^{jk|\mathbf{r}'-\mathbf{r}|}}{|\mathbf{r}'-\mathbf{r}|}. \tag{4}$$

The target scatters the incident wave, whose potential is denoted by U^{in} and is given in (3), from the transmitter, and generates a secondary charge source $Q'(\mathbf{r})$, where $\mathbf{r} \in \Omega_o$, as illustrated in Fig. 1. For penetrable scatters, the induced source due to the incident wave is determined by

$$Q'(\mathbf{r}) = V(\mathbf{r})U^{in}(\mathbf{r}), \tag{5}$$

where V is called the scattering potential which is determined by the material of the target. For simplicity, we assume that V is independent of the frequency w, which means that the target is colorless. The resulting field U is determined by the following Lippmann-Schwinger equation:

$$U(\mathbf{r}) = U^{in}(\mathbf{r}) + \int_{\Omega_o} G_{0+}(\mathbf{r}-\mathbf{r}')V(\mathbf{r}')U(\mathbf{r}')d\mathbf{r}', \tag{6}$$

where G_{0+} is the Green function for the outgoing EM wave upon scattering. The explicit expression of G_{0+} is very difficult to calculate, even for simple shapes of the target. For simplicity of analysis, we adopt the Bonn's approximation [15] and assume $G_{0+} = G_+$, namely omitting the coupling effect of the transceiver and target. Then, the solution to (6) is given by

$$U(\mathbf{r},w) = U^{in}(\mathbf{r},w) + \int_{\Omega_o} G_+(\mathbf{r}-\mathbf{r}')V(\mathbf{r}')U^{in}(\mathbf{r}',w)d\mathbf{r}', \tag{7}$$

which maps from the incident wave U^{in} to the final scattered wave U'.

III. EM Field Analysis on Radar Imaging

In this section, we analyze the performance of radar imaging, based on the EM field model in Section II.

A. Received Signal

We first consider a single-tone source with frequency w. Hence, the argument of frequency w can be omitted for notational simplicity. Suppose that the radar transmitter and receiver are well insulated, such that the term U^{in} in the Lippmann-Schwinger equation in (6) can be omitted. The

signal at the receiver, scattered back from the target, is given by (assuming the Bonn's approximation)

$$S'(\mathbf{r}) = \int_{\Omega_o} G_+(\mathbf{r}-\mathbf{r}')V(\mathbf{r}')U(\mathbf{r}')d\mathbf{r}', \tag{8}$$

where U is the incident wave U^{in} in (7) and is determined by (3). We assume Gaussian noise in the measurement. Therefore, the measurement at position $\mathbf{r}$ is given by $S(\mathbf{r}) = S'(\mathbf{r}) + N(\mathbf{r})$. Here N forms a Gaussian random field. We assume N is unbiased (i.e., $E[N(\mathbf{r})] = 0$) and denote $E[N^*(\mathbf{r})N(\mathbf{r}')] = \Sigma(\mathbf{r},\mathbf{r}')$. Moreover, we assume $E[N(\mathbf{r})N(\mathbf{r}')] = 0$. Note that Σ is a bi-variant function and can also be considered as a Kernel.

B. Imaging Error Analysis

We analyze the performance by calculating the Fisher information operator and the corresponding Cramer-Rao bound.

1) Fisher Information Operator: For the imaging task, we can consider the unknown $V(\mathbf{r})$ as the parameters. For parameter estimations, the fundamental tool is the Fisher information matrix. However, in the setup of this paper, the parameter $V(\mathbf{r})$ is continuous in the space, as a function instead of a number. Therefore, the Fisher information is an operator, instead of a finite dimensional matrix. Similarly to the traditional Fisher information, we define the Fisher information operator $\mathcal{I}$ by

$$\mathcal{I}f(\mathbf{r}) = \int_{\Omega_o} K(\mathbf{r},\mathbf{r}')f(\mathbf{r}')d\mathbf{r}', \tag{9}$$

where f is a function over Ω_o, and the kernel K is given by

$$K(\mathbf{r},\mathbf{r}') = E\left[\left(\delta_{V(\mathbf{r})}\log p(S|V)\right)^*\delta_{V(\mathbf{r}')}\log p(S|V)\right], \tag{10}$$

where $\mathbf{r}$ and $\mathbf{r}'$ in Ω_o can be considered as the indices, and the Frechét derivative $\delta_{V(\mathbf{r})}$ for functional F is given by

$$\delta_{V(\mathbf{r})}F(V) = \lim_{h\to 0}\frac{F(V+h\delta_{\mathbf{r}}) - F(V)}{h}, \tag{11}$$

where $\delta_{\mathbf{r}}$ is the delta function of position $\mathbf{r}$.

The Fisher information operator is obtained in the following theorem, whose proof is omitted due to limited space.

Theorem 1: Given the received signal model of radar sensing, the kernel of the Fisher information operator is given by

$$\begin{aligned} K(\mathbf{r},\mathbf{r}') &= \frac{1}{2}Re\left[U(\mathbf{r})U^*(\mathbf{r}')\int_{\Omega_x^2} G_+(\mathbf{r}_1-\mathbf{r})G_+^*(\mathbf{r}_3-\mathbf{r}')\right. \\ &\times \left.\Sigma^{-1}(\mathbf{r}_1,\mathbf{r}_3)d\mathbf{r}_1 d\mathbf{r}_3\right]. \end{aligned} \tag{12}$$

When the noise is independent in the space, we have $\Sigma(\mathbf{r_1},\mathbf{r_2}) = \sigma_n^2\delta(\mathbf{r}_1-\mathbf{r}_2)$. Then, we obtain the simplified Fisher information operator in the following corollary.

Corollary 1: For the spatially independent noise, the kernel of the Fisher information operator is given by

$$\begin{aligned} K(\mathbf{r},\mathbf{r}') &= \frac{1}{2\sigma_n^2}Re\left[U(\mathbf{r})U^*(\mathbf{r}')\right. \\ &\times \left.\int_{\Omega_x} G_+(\mathbf{r}_1-\mathbf{r})G_+^*(\mathbf{r}_1-\mathbf{r}')d\mathbf{r}_1\right]. \end{aligned} \tag{13}$$

For simplicity of analysis, in the subsequent analysis, we assume spatially independent noise. Then, the Fisher information operator $\mathcal{I}$ is determined by

$$\begin{aligned} \mathcal{I}f(\mathbf{r}) &= \frac{U(\mathbf{r})}{\sigma_n^2}\int_{\Omega_x}d\mathbf{r}_1\int_{\Omega_o}d\mathbf{r}'G_+(\mathbf{r}_1-\mathbf{r})G_+^*(\mathbf{r}_1-\mathbf{r}') \\ &\times U^*(\mathbf{r}')f(\mathbf{r}'), \qquad \forall\mathbf{r}\in\Omega_o, \end{aligned} \tag{14}$$

where f is supported on Ω_o.

2) Cramer-Rao Bound: The Cramer-Rao bound states that

$$\int_{\Omega_o} E\left[(\hat{V}(\mathbf{r}) - V(\mathbf{r}))^2\right]d\mathbf{r} \geq \int_{\Omega_o} K^{-1}(\mathbf{r},\mathbf{r})d\mathbf{r}, \tag{15}$$

where $\hat{V}$ is the estimation of V, the left hand side is the MSE of sensing, and K^{-1} in the right hand side is the kernel of the inverse operator $\mathcal{I}$. Then, we need the spectral decomposition for the Fisher information operator $\mathcal{I}$, since

$$\int_{\Omega_o} K^{-1}(\mathbf{r},\mathbf{r})d\mathbf{r} = \int_0^\infty \frac{1}{\lambda}d\mu_\lambda^I, \tag{16}$$

where λ is the eigenvalue of the operator $\mathcal{I}$ and μ_λ^I is the measure of the corresponding eigenvalues of $\mathcal{I}$. Since $\mathcal{I}$ is Hermitian and positive definite, we have $\lambda > 0$. Then, the problem boils down to the evaluation of the eigenvalues of the Fisher information operator $\mathcal{I}$.

C. Eigen-decomposition of $\mathcal{I}$

1) Identical U: We first assume that U is identical within Ω_o such that $|U(\mathbf{r})|^2 = P$, which is reasonable when the target is small. Then, the Fisher information operator is given by

$$\mathcal{I}Q(\mathbf{r}) = \frac{P}{\sigma_n^2}\int_{\Omega_x}\int_{\Omega_o} G_+(\mathbf{r}_1,\mathbf{r})G_+^*(\mathbf{r}_1,\mathbf{r}')Q(\mathbf{r}')d\mathbf{r}_1 d\mathbf{r}'. \tag{17}$$

When Q is an eigenfunction of the linear operator $\mathcal{I}$, we have $\mathcal{I}Q(\mathbf{r}) = \lambda Q(\mathbf{r})$, where λ is the eigenvalue corresponding to Q. We consider the special cases in which the Green function can be written as

$$G_+(\mathbf{r},\mathbf{r}') = \sum_{k=0}^{\infty}\psi_k(\mathbf{r})\phi_k(\mathbf{r}'), \tag{18}$$

where both $\{\phi_k\}_k$ and $\{\psi_k\}_k$ form basis of the functions over $\mathbb{R}^3$. Now, suppose that the j-th eigenfunction of $\mathcal{I}$, denoted by η_k and associated with eigenvalue λ_k, is $\eta_k(\mathbf{r}) = \sum_{j=0}^{\infty} a_j^k\phi_j(\mathbf{r})$, where the coefficients $\{a_j^k\}_j$ and

the eigenvalue λ_k are to be determined. Since the η_k is the eigenfunction, we have

$$\mathcal{I}\eta_k(\mathbf{r}) = \lambda_k \eta_k(\mathbf{r}), \qquad \forall \mathbf{r} \in \Omega_o. \tag{19}$$

Substituting the above decompositions into (19) and calculating $\mathcal{I}\eta_k$, we have

$$\begin{aligned} \mathcal{I}\eta_k(\mathbf{r}) &= \frac{P}{\sigma_n^2} \sum_{k_1=0}^{\infty} \phi_{k_1}(\mathbf{r}) \sum_{k_2,k_3=0}^{\infty} \int_{\Omega_x} d\mathbf{r}_1 \int_{\Omega_o} d\mathbf{r}' \\ &\quad \psi_{k_1}(\mathbf{r}_1)\psi^*_{k_2}(\mathbf{r}_1)\phi^*_{k_2}(\mathbf{r}')a^k_{k_3}\phi_{k_3}(\mathbf{r}')d\mathbf{r}' \\ &= \sum_{k_1=0}^{\infty} \left(\sum_{k_3=0}^{\infty} c_{k_1,k_3} a^k_{k_3} \right) \phi_{k_1}(\mathbf{r}), \end{aligned} \tag{20}$$

where the coefficients c_{k_1,k_3} is given by

$$\begin{aligned} c_{k_1,k_3} &= \sum_{k_2=0}^{\infty} \int_{\Omega_x} d\mathbf{r} \int_{\Omega_o} d\mathbf{r}' \\ &\quad \psi_{k_1}(\mathbf{r})\psi^*_{k_2}(\mathbf{r})\phi^*_{k_2}(\mathbf{r}')\phi_{k_3}(\mathbf{r}'). \end{aligned} \tag{21}$$

By comparing (19) and (20), we have $\sum_{k_3=0}^{\infty} c_{k_1,k_3} a^k_{k_3} = \lambda_k a^k_{k_1}$, which can be written in the matrix form:

$$\mathbf{C}\mathbf{a}^k = \lambda_k \mathbf{a}^k, \tag{22}$$

where $\mathbf{C} = (c_{mn})_{mn}$ and $\mathbf{a}^k = (a^k_0, a^k_1, a^k_2, ...)$. Then, the eigenvalue λ_k is actually the k-th eigenvalue of the infinite dimensional matrix $\mathbf{C}$.

If we further have the following orthogonality

$$\int_{\Omega_o} \phi^*_{k_2}(\mathbf{r}')\phi_{k_3}(\mathbf{r}')d\mathbf{r}' = C_{\Omega_0}\delta_{k_2,k_3}, \tag{23}$$

where C_{Ω_0} is a constant dependent on Ω_o, the coefficient c_{k_1,k_3} can be further simplified to

$$c_{k_1,k_3} = \int_{\Omega_x} \psi_{k_1}(\mathbf{r}_1)\psi^*_{k_3}(\mathbf{r}_1)d\mathbf{r}_1. \tag{24}$$

Given the above assumptions, the Cramer-Rao bound of MSE is given by

$$MSE = \sum_k \frac{\sigma_n^2}{\lambda_k^2(\{c_j\}_j)P}, \tag{25}$$

where we emphasize that the eigenvalue λ_k is a function of the eigenvalues $\{c_j\}_j$ of the Green function.

2) Generic U: For the generic case of U, we assume that (18) holds. Then, we can define

$$\tilde{G}_+(\mathbf{r}, \mathbf{r}') = G_+(\mathbf{r}, \mathbf{r}')U(\mathbf{r}'). \tag{26}$$

The new Green function $\tilde{G}_+$ has the following decomposition, which is similar to (18):

$$\tilde{G}_+(\mathbf{r}, \mathbf{r}') = \sum_{k=0}^{\infty} \psi_k(\mathbf{r})\tilde{\phi}_k(\mathbf{r}'), \tag{27}$$

where $\tilde{\phi}_k(\mathbf{r}') = \phi_k(\mathbf{r}')U(\mathbf{r}')$. Then, we simply repeat the above argument using the new Green function $\tilde{G}_+$ and the new basis function $\{\tilde{\phi}_k\}_k$. As we will see, for the spherical coordinates, we can further simplify the analysis by exploiting the property of spherical harmonic functions.

D. Spherical Coordinate Case

We consider the sphere coordinates and the corresponding expansion of the Green function. We assume that the target is a sphere centered at the origin and the radius is given by R. It is well known that the outgoing-wave Green function can be represented by the following multipole expansion [15]:

$$G(\mathbf{r}, \mathbf{r}') = -jk \sum_{l=0}^{\infty} \sum_{m=-l}^{l} j_l(kr_<)h_l^+(kr_>)Y_l^m(\hat{\mathbf{r}})Y_l^{m*}(\hat{\mathbf{r}}'), \tag{28}$$

where the notation is as follows:

- $k = \frac{2\pi}{\lambda}$ is the wavenumber.
- $r = \|\mathbf{r}\|$, $\hat{\mathbf{r}} = \frac{\mathbf{r}}{r}$, $r_< = \min\{r, r'\}$, $r_> = \max\{r, r'\}$.
- j_l is the l-th order spherical Bessel function given by $j_l(z) = \sqrt{\frac{\pi}{2kr}} J_{l+\frac{1}{2}}(z)$, where $J_{l+\frac{1}{2}}$ is the ordinary Bessel function.
- h_l is the spherical Hankel function and is defined as $h_l(z) = j_l(z) + jn_l(z)$, where $n_l(z)$ is the spherical Neumann function and is defined as $n_l(kr) = \sqrt{\frac{\pi}{2kr}} N_{l+\frac{1}{2}}(kr)$ (N is the ordinary Neumann function).
- Y_l^m is the spherical harmonics function, defined as

$$\begin{aligned} &Y_l^m(\theta, \phi) \\ &= (-1)^m \sqrt{\frac{2l+1}{4\pi}\frac{(l-m)!}{(l+m)!}} P_l^m(\cos\theta)e^{km\phi}, \end{aligned} \tag{29}$$

  where P_l^m is the Legendre polynomial.

In our context, since $\mathbf{r}' \in \Omega_o$ and $\mathbf{r} \in \Omega_x$ (hence $r' < r$), we can simplify (28) to

$$G(\mathbf{r}, \mathbf{r}') = -jk \sum_{l=0}^{\infty} \sum_{m=-l}^{l} j_l(kr')h_l^+(kr)Y_l^m(\hat{\mathbf{r}})Y_l^{m*}(\hat{\mathbf{r}}'). \tag{30}$$

Due to the limited space, we consider only the case of equal U and leave the generic case of U to our full version. We assume that Ω_o is a sphere and U is identical within Ω_o. Then, we define the following eigenfunctions:

$$\begin{cases} \psi_{l,m}(\mathbf{r}) = -jkh_l^+(kr)Y_l^m(\hat{\mathbf{r}}) \\ \phi_{l,m}(\mathbf{r}') = j_l(kr')Y_l^{m*}(\hat{\mathbf{r}}') \end{cases}, \tag{31}$$

where the subscript is described by two integers. Since the spherical harmonics function is orthogonal with respect to a spherical region, namely (Eq. (3.31) in [15])

$$\int_{\Omega_o} Y_l^m(\theta, \phi)Y_{l'}^{m'*}(\theta, \phi)d\theta d\phi = \delta_{l,l'}\delta_{m,m'}, \tag{32}$$

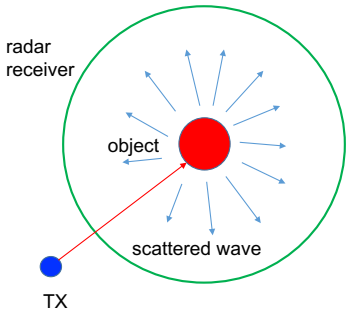

Fig. 2: Illustration of sphere radar receiver.

(23) is valid, which simplifies the expression of $\mathbf{C}$ in (22) to

$$c_{(l,m),(l',m')} = k^2 \int_{\Omega_o} |j_l(kr')|^2 \, dr' \times \int_{\Omega_x} h_l^+(kr) h_{l'}^{+*}(kr) Y_l^m(\hat{\mathbf{r}}) Y_{l'}^{m'*}(\hat{\mathbf{r}}) d\mathbf{r}. \quad (33)$$

For a generic shape of Ω_x, the expression $c_{(l,m),(l',m')}$ can no longer be simplified.

When Ω_x is a 2-dimensional sphere around the target with radius R, as illustrated in Fig. 2, by applying (32), $c_{(l,m),(l',m')}$ can be further simplified to

$$c_{(l,m),(l',m')} = \pi k^2 R^2 |h_l^+(kR)|^2 \times \int_{\Omega_o} |j_l(kr')|^2 \, dr' \delta_{l,l'} \delta_{m,m'}. \quad (34)$$

The eigenvalues are given by

$$\lambda_l = \pi k^2 R^2 |h_l^+(kR)|^2 \int_{\Omega_o} |j_l(kr')|^2 \, dr'. \quad (35)$$

This situation is reasonable in the context of distributed radar system, in which one transmitter provides illuminating EM wave while multiple receivers around the target pick up the scattered wave for imaging.

IV. EM Field Analysis on Communications

In this section, we study the capacity of data communications using the EM field analysis.

A. EM Field Channel

For simplicity, we ignore scatterers (including the radar target) and consider a free space propagation for the communication signal. The input-output relationship for data communications is given by

$$U(\mathbf{r}, w) = \int_{\Omega_t} G_+(\mathbf{r}', \mathbf{r}) Q(\mathbf{r}', w) d\mathbf{r}, \qquad \mathbf{r} \in \Omega_r, \quad (36)$$

where Q and U are the input and output, respectively. The alphabets of the input and output are $L^2(\Omega_t)$ and $L^2(\Omega_r)$, respectively. Therefore, the communication channel is essentially the linear operator G induced by the integral transform. We further assume that the observation at the receiver antenna is contaminated by additive white Gaussian noise.

B. Channel Capacity

For simplicity of analysis, we assume that all the EM wave power is absorbed by the aperture, which is subject to Gaussian noise. Therefore, the received signal is represented by $\tilde{U}(\mathbf{r}) = U(\mathbf{r}) + N(\mathbf{r})$, where N is the noise filed on the target. We further assume that $U(\mathbf{r})$ is a Gaussian field with spatial independence.

Using the same argument as that in [16], by extending the results from Gaussian process to Gaussian field,

Theorem 2: For a single frequency w, we have

$$C(w) = \sum_{i=1}^{\infty} \log_2 \left(1 + \frac{P_k(w)\lambda_k(w)}{\sigma_n^2}\right), \quad (37)$$

where σ_n^2 is the noise power and λ_k is the k-th eigenvalue of the following operator $\mathcal{T}$:

$$\mathcal{T} f(\mathbf{r}) = \int_{\Omega_o} E\left[U(\mathbf{r}) U^*(\mathbf{r}')\right] f(\mathbf{r}') d\mathbf{r}', \quad (38)$$

where the expectation is over the randomness of the source charge Q.

V. Numerical Results

In this section, we provide numerical results to illustrate the above theoretical analysis.

A. System Setup

We consider a transmitter at the origin, an target located at $[200m, 0m, 0m]$ and a communication receiver located at $[0m, 0m, 200m]$. We consider the 77GHz band for JCR, where a bandwidth of 400M is used. The transmit power is set to 12dBm while the noise PSD is -174dBm/Hz.

B. MSE-Capacity Trade-off

1) Separate Operations: We tested the case in which radar and communications are operated in different frequency bands; thus the transmit power is also divided between communications and radar. We consider a 20×20 uniform grid to the power-bandwidth rectangle and evaluate the performance (channel capacity and sensing MSE) for each point (corresponding to one scheme of power-bandwidth division between communications and radar) in the grid. The points representing the performances are plotted in the capacity-MSE plane in Fig. 3. The points characterizes the feasible region of the JCR performance. One observation is that the region is convex, which is essentially due to the marginal performance gain when more power and bandwidth are allocated to communications or radar.

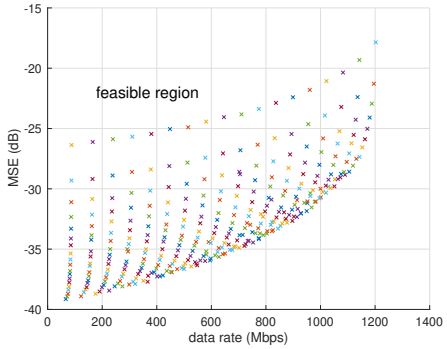

Fig. 3: Trade-off between communications and radar for separate operations.

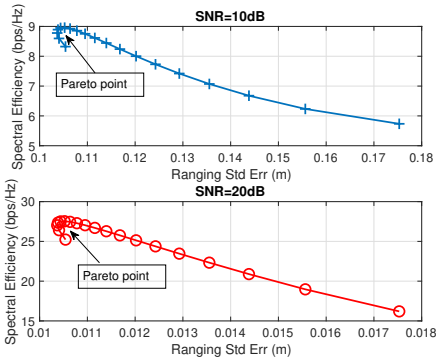

Fig. 4: Trade-off for joint communications and radar sensing.

2) Joint Operations: We assume that the field U consists of the first order and second order spherical harmonics, namely $u_l^m = 0$ when $l \geq 3$. We further assume that the power is identically distributed in u_l^m, $m = -l, ..., l$, namely for each mode of order l. We assume $R_o = 0.3m$ and $R_x = 20m$. The coefficients $c(l_1, m_1, l_2, m_2)$ are calculated for l_1 and l_2 ranging from 1 to 20 . The numerical results show that the first coefficient $c(1, 0, 1, 0)$ dominates others. Therefore, we approximate the eigenvalue by $1/c(1, 0, 1, 0)$. Meanwhile, due to the orthogonality of the modes (l_1, m_1) and (l_2, m_2), the communication spectral efficiency (in bps/Hz) is given by

$$C = 2\log_2\left(1 + \frac{|u_{11}|^2 P}{N_0 W}\right) + 5\log_2\left(1 + \frac{|u_{21}|^2 P}{N_0 W}\right). \quad (39)$$

Then, we range the power proportion of the first-order harmonics from 0.05 to 0.95, and plot the corresponding ranging error and communication spectral efficiency, for the cases of SNR=10dB and 20dB, respectively. The results are shown in Fig. 4. We observe that there is only a single Pareto point, which is the most upper-left one, namely moving from it implies the worse off of at least one function. Other points are dominated by this operational state. It implies the possibility of other Pareto points when more orders and modes of U are taken into account. It also shows the complexity of the trade-off between communications and radar sensing, since the Pareto boundary needs higher orders and more modes of the field.

VI. Conclusions

In this paper, we have analyzed the performance trade-off between communications and radar when they share the same waveform in an inseparable manner. We have considered the spherical harmonics decomposition for the spherical coordinates, from which we have derived the Cramer-Rao bound and channel capacity. Numerical computations have been conducted, which have shown the Pareto point for a certain setup, as well as the complexity of the trade-off boundary.

References

[1] A. R. Chiriyath, B. Paul, G. M. Jacyna, and D. W. Bliss, "Inner bounds on performance of radar and communications co-existence," *IEEE Transactions on Signal Processing*, vol. 64, no. 2, pp. 464–474, 2015.

[2] A. R. Chiriyath, B. Paul, and D. W. Bliss, "Radar-communications convergence: Coexistence, cooperation, and co-design," *IEEE Transactions on Cognitive Communications and Networking*, vol. 3, no. 1, pp. 1–12, 2017.

[3] L. Zheng, M. Lops, X. Wang, and E. Grossi, "Joint design of overlaid communication systems and pulsed radars," *IEEE Transactions on Signal Processing*, vol. 66, no. 1, pp. 139–154, 2017.

[4] L. Zheng, M. Lops, and X. Wang, "Adaptive interference removal for uncoordinated radar/communication coexistence," *IEEE Journal of Selected Topics in Signal Processing*, vol. 12, no. 1, pp. 45–60, 2017.

[5] M. S. L. A. Y. Fan, J. Bao and H. Li, "Communications via frequency-modulated continuous-wave radar in millimeter wave band," in *Proc. of IEEE International Global Communications Conference*, 2019.

[6] B. Paul, A. R. Chiriyath, and D. W. Bliss, "Survey of rf communications and sensing convergence research," *IEEE Access*, vol. 5, pp. 252–270, 2016.

[7] L. Zheng, M. Lops, Y. C. Eldar, and X. Wang, "Radar and communication co-existence: an overview," *arXiv preprint arXiv:1902.08676*, 2019.

[8] F. Liu, C. Masouros, A. Petropulu, H. Griffiths, and L. Hanzo, "Joint radar and communication design: Applications, state-of-the-art, and the road ahead," *IEEE Transactions on Communications*, 2020.

[9] D. Ma, N. Shlezinger, T. Huang, Y. Liu, and Y. C. Eldar, "Joint radar-communications strategies for autonomous vehicles," *IEEE Signal Processing Magazine*, vol. 37, no. 4, pp. 85–97, 2020.

[10] O. M. Bucci and G. Franceschetti, "On the spatial bandwidth of scattered fields," *IEEE Transactions on Antennas and Propagation*, vol. 35, no. 12, pp. 1445–1455, 1987.

[11] ——, "On the degrees of freedom of scattered fields," *IEEE Transactions on Antennas and Propagation*, vol. 37, no. 7, pp. 918–926, 1989.

[12] M. D. Migliore, "On electromagenetics and information theory," *IEEE Transactions on Antennas and Propagation*, vol. 56, no. 10, pp. 3188–3200, 2008.

[13] M. Franceschetti, M. D. Migliore, and P. Minero, "The capacity of wireless networks: Information-theoretic and physical limits," *IEEE Trans. on Information Theory*, vol. 55, no. 8, pp. 3413–3420, 2009.

[14] M. Franceschetti, M. D. Migliore, P. Minero, and F. Schettino, "The degrees of freedom of wireless networks via cut-set integral," *IEEE Transactions on Information Theory*, vol. 57, no. 5, pp. 3067–3079, 2011.

[15] A. J. Devaney, *Mathematical Foundations of Imaging, Tomography and Wavefield Inversion*. Cambridge University Press, 2012.

[16] S. Ihara, *Information Theory for Continuous Systems*. World Scientific, 1993.